RSC Advances

PAPER

View Article Online
View Journal | View Issue

Cite this: *RSC Adv.*, 2014, **4**, 9383

Coordination behaviour of new dipyridylpyrazole ligands towards $ZnCl_2$ and $PdCl_2$ fragments. Crystalline structural characterization and multinuclear NMR studies as evidence of linkage and conformational isomers†‡

Lorena Soria,[a] Paloma Ovejero,[a] Mercedes Cano,*[a] José Vicente Heras,§[a] M. Rosario Torres,[b] Rosa Claramunt[c] and Pilar Cornago[c]

A series of novel *N,N,N*-donor pyrazole based ligands of the type $pypz^{R(n)py}$ (R(*n*) = $C_6H_4OC_nH_{2n+1}$, *n* = 1, 12–18) (**1–5**) bearing two pyridine substituents at the 1- and 3-positions and an alkyloxyphenyl group at the 5-position have been prepared and characterized. The X-ray structure of $pypz^{R(1)py}$ is presented. Coordination of those ligands to MCl_2 fragments (M = Zn, Pd) gives rise to complexes of the type $[MCl_2(pypz^{R(n)py})]$ (M = Zn, Pd; R(*n*) = $C_6H_4OC_nH_{2n+1}$; *n* = 1, 12–18) (**6–15**) which were characterized and studied in the solid state and in solution. In these compounds the ligands were highly versatile as they were metal coordinated in a *N,N*-bidentate, *N,N,N*-tridentate fashion or *N,N*-bidentate fashion with an additional interaction *via* the third active nitrogen, this different behaviour depending on the metal fragment as well as on the state (solid or in solution) in which the complexes are. The X-ray structures of $[ZnCl_2(pypz^{R(1)py})]$ (**6**) and $[PdCl_2(pypz^{R(1)py})]$ (**11**) have also been determined showing distorted trigonal bipyramid and square-planar geometries at the zinc and palladium centres, respectively. In both cases the coordination environment has been confirmed by ^{13}C-and ^{15}N-NMR studies in solid state. In particular, two binuclear M–M stereoisomers "Z"- and "U"-shaped may be established for the Pd derivative. The ^1H and ^{13}C-NMR studies in $CDCl_3$ solution of (**6**) and (**11**) indicate the presence of monomeric species which exhibit the same or different bidentate coordination of the ligand, respectively, than that observed in solid state. However, DMSO-d^6 causes a total dissociation of the ligand in Zn derivatives, while for the related Pd complexes two monomeric linkage isomers (N2,N1′PdCl2 and N2,N1′′PdCl2) were detected.

Received 14th October 2013
Accepted 20th January 2014

DOI: 10.1039/c3ra45821k

www.rsc.org/advances

Introduction

The interest of the current research on metallomesogens is directed to explore new systems with optimized LC properties.[1,2]

In this context, factors such as coordination geometry, the nature of the metal fragments or the characteristics of the ligands have been investigated in many metal derivatives.

In particular in our research group, many metallomesogens containing mesogenic or promesogenic pyrazole type ligands have been prepared.[3–6] In addition, we have found that the introduction of a polar group like pyridine on the molecular periphery appears to be determinant to achieve and/or to improve the mesomorphic properties of the metal complexes.[7] So it was interesting to note that Ag(I) and Pd(II) metallomesogens with pyridylpyrazole type ligands $pypz^{R(n)}$ and $Hpz^{R(n)py}$ (R(*n*) = $C_6H_4OC_nH_{2n+1}$, *n* = 1, 12–18)[3–6] exhibited lower melting points and a wider mesophase range than the related ones with ligands not containing pyridine groups.[4,7] On the other hand dipyridylpyrazole ligands have been recently proved as candidates to stabilize polymeric structures through strong chelation.[8–14] Therefore they could play a significant role as inducers of LC behaviour. On these basis we propose to explore the potential ability of new related long-chained ligands to generate metallomesogens.

The present paper reports the synthesis and characterisation of a new versatile class of alkyloxyphenyl-substituted dipyridylpyrazoles $pypz^{R(n)py}$ (R(*n*) = $C_6H_4OC_nH_{2n+1}$, *n* = 1, 12–18)

[a]*Departamento de Química Inorgánica I, Facultad de Ciencias Químicas, Universidad Complutense, 28040 Madrid, Spain. E-mail: mmcano@quim.ucm.es; Fax: +34 91 394 4352; Tel: +34 91 394 4340*

[b]*CAI de Difracción de Rayos-X, Facultad de Ciencias Químicas, Universidad Complutense, 28040 Madrid, Spain. E-mail: mrtorres@quim.ucm.es; Tel: +34 91 394 4284*

[c]*Departamento de Química Orgánica, Facultad de Ciencias, UNED, 28040, Madrid, Spain. E-mail: rclaramunt@ccia.uned.es*

† Dedicated to the memory of Prof.Dr José Vicente Heras Castelló.

‡ Electronic supplementary information (ESI) available. CCDC 948534 (**1**), 948535 (**6**) and 948536 (**11**). For ESI and crystallographic data in CIF or other electronic format see DOI: 10.1039/c3ra45821k

§ Deceased on 26th April, 2013.

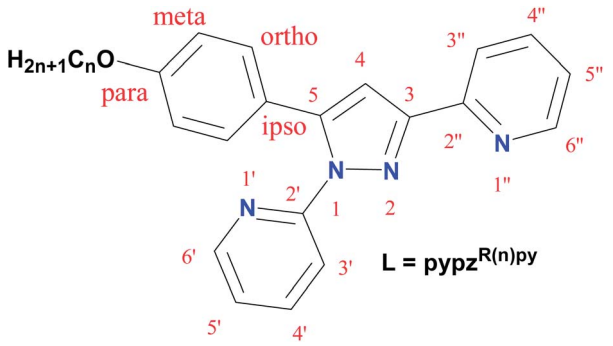

Fig. 1 Schematic representation and numbering of the atoms for $pypz^{R(n)py}$ ligands.

(**1–5**) (Fig. 1) as well as the study of their metal complexes of the type $[MCl_2(pypz^{R(n)py})]$ (M = Zn, Pd, R(n) = $C_6H_4OC_nH_{2n+1}$, n = 1, 12–18) (**6–15**) (Table 2). A careful structural analysis of the coordination compounds will be achieved in order to establish structure/properties relationship.

Experimental

Materials and physical measurements

All commercial reagents were used as supplied. Elemental analysis for carbon, hydrogen and nitrogen were carried out by the Microanalytical Service of Complutense University. IR spectra were recorded on a FTIR Thermo Nicolet 200 spectrophotometer in solid state, with samples as KBr pellets, in the 4000–400 cm^{-1} region.

Solution NMR spectra

Solution NMR spectra of **1**, **6** and **11** were recorded on a Bruker DRX 400 (9.4 T; 400.13 MHz for ^1H, 100.62 MHz for ^{13}C and 40.56 MHz for ^{15}N) spectrometer fitted with a 5 mm inverse detection H–X probe and equipped with a z-gradient coil at 300 K. ^1H and ^{13}C NMR chemical shifts (δ in ppm) are referenced to Me_4Si; for ^{15}N NMR, nitromethane (0.00) was used as an external standard. Typical parameters for ^1H NMR spectra were: spectral width 3100 Hz and pulse width 7.5 μs at an attenuation level of 0 dB. Typical parameters for ^{13}C NMR spectra were: spectral width 21 kHz, pulse width 10.6 μs at an attenuation level of −6 dB and relaxation delay 2 s. 2D (^1H–^{13}C) gs-HMQC and, (^1H–^{13}C) gs-HMBC were acquired and processed using standard Bruker NMR software and in non-phase-sensitive mode. Selected parameters for (^1H–^{13}C) gs-HMQC and gs-HMBC spectra were spectral width 3100 Hz for ^1H and 25 kHz for ^{13}C, 1024 × 256 data set, number of scans 2 (gs-HMQC) or 4 (gs-HMBC) and relaxation delay 1 s. The FIDs were processed using zero filling in the F1 domain and a sine-bell window function in both dimensions was applied prior to Fourier transformation. In the gs-HMQC experiments GARP modulation of ^{13}C was used for decoupling. ^{15}N NMR spectra were acquired using 2D inverse proton detected heteronuclear shift correlation spectroscopy. Typical parameters for the gs-HMBC (^1H–^{13}C) spectra were: a spectral width of 3100 Hz for ^1H and 12.5 kHz for ^{15}N, a 1024 × 256 data set, a relaxation delay of 1 s and a 7 ms delay for the using zero filling in the F1 domain, and a sine-bell window function in both dimensions was applied prior to Fourier transformation.

For the rest of compounds ^1H-NMR spectra were performed at room temperature on a Bruker DPX-300 spectrophotometer (NMR Service of Complutense University) from solutions in DMSO-d^6 or $CDCl_3$. ^1H Chemical shifts (δ) are listed relative to Me_4Si using the signal of the deuterated solvent as reference (2.50 and 7.26 ppm, respectively), and coupling constants J are in hertz. Multiplicities are indicated as s (singlet), d (doublet), t (triplet), dd (doublet of doublets), ddd (double doublet of doublets) and m (multiplet). The ^1H chemical shifts and coupling constants are accurate to ±0.01 ppm and ±0.3 Hz, respectively.

Solid state

Solid-state ^{13}C (100.73 MHz) and ^{15}N (40.60 MHz) CPMAS NMR spectra of 1, 6 and 11 have been obtained on a Bruker WB 400 spectrometer at 300 K using a 4 mm DVT probehead. Samples were carefully packed in a 4 mm diameter cylindrical zirconia rotor with Kel-F end-caps. Operating conditions involved 3.2 μs 90° ^1H pulses and decoupling field strength of 78.1 kHz by TPPM sequence. ^{13}C spectra were originally referenced to a glycine sample and then the chemical shifts were recalculated to the Me_4Si [for the carbonyl atom δ (glycine) = 176.1 ppm]. Similarly, ^{15}N spectra were initially referenced to $^{15}NNH_4Cl$ and then recalculated to nitromethane, using the relationship δ ^{15}NNitromethane = δ $^{15}NNH_4Cl$ − 338.1. Typical acquisition parameters for ^{13}C CPMAS were: spectral width, 40 kHz; recycle delay, 5 s; acquisition time, 30 ms; contact time, 2 ms; and spin rate, 12 kHz. In order to distinguish protonated and unprotonated carbon atoms, the NQS (Non-Quaternary Suppression) experiment by conventional cross-polarization was recorded; before the acquisition the decoupler is switched off for a very short time of 25 μs. Typical parameters for the ^{15}N CPMAS were: spectral width, 40 kHz; recycle delay, 5 s, acquisition time, 35 ms; contact time, 7 ms; and spin rate, 6 kHz. Fig. 1 recovers the nomenclature used in the NMR assignments.

Phase studies were carried out by optical microscopy using an Olympus BX50 microscope equipped with a Linkam THMS 600 heating stage. The temperatures were assigned on the basis of optic observations with polarised light.

Compounds 1,3-bis-(2-pyridyl)-5-(4-*n*-alkyloxyphenyl)pyrazole [$pypz^{R(n)py}$] (R(n) = $C_6H_4OC_nH_{2n+1}$, n = 1, 12–18) (1–5)

To a solution of 6.1 mmol of the corresponding β-diketone (synthesised according to the previously described methods)[15] in 200 mL of absolute ethanol were added 2 mL of HCl (35%) and 9.5 mmol of NH_2NHpy (97%). The reaction mixture was stirred for 72 h at reflux temperature. Once it was cooled to room temperature, 50 mL of a saturated Na_2CO_3 aqueous solution was added until neutral pH was reached, being observed, at this point, the plentiful appearance of a brown precipitate, which was filtered off and washed with 50 mL of CH_2Cl_2. The solution was extracted with CH_2Cl_2 (2 × 50 mL) and

the organic layers were washed with water (2 × 50 mL) and dryed over anhydrous $MgSO_4$. The solvent of the resulting brown/orange solution was removed under the reduced pressure of a rotatory evaporator until the formation of an oily product which was dissolved with 15 mL of diethyl ether. The final solid was formed by slow evaporation of the solvent at room temperature.

[pypz$^{R(1)py}$]·H$_2$O (1). Yellow solid (60%). Elemental analysis: found: C, 69.9; H, 5.4; N, 15.9%. $C_{20}H_{16}N_4O$ requires C, 69.4; H, 5.2; N, 16.2%. ν_{max}(KBr)/cm^{-1}: 1614 ν(C=C + C=N), 782 $\gamma(CH)_{py}$. δ_H (see Results and discussion section).

[pypz$^{R(12)py}$] (2). Dark brown solid (73%). Elemental analysis: found: C, 75.9; H, 7.6; N, 12.4%. $C_{31}H_{38}N_4O$ requires C, 77.1; H, 7.9; N, 11.6%. ν_{max}(KBr)/cm^{-1}: 1614 ν(C=C + C=N), 786 $\gamma(CH)_{py}$. δ_H (300 MHz, DMSO-d^6, Me_4Si)/ppm: 0.85 (t, ^3J 6.8, 3H, CH_3), 1.24 (m, 18H, CH_2), 1.68 (m, 2H, CH_2), 3.95 (t, ^3J 6.4, 2H, OCH_2), 6.88 (d, ^3J 8.8, 2H, H_m), 7.13 (s, 1H, H4), 7.19 (d, ^3J 8.8, 2H, H_o), 7.39 (ddd, ^3J 7.4, ^3J 4.8, ^4J 1.1, 1H, H5′), 7.46 (ddd, ^3J 7.4, ^3J 4.9,^4J 1.0, 1H, H5″), 7.73 (d, ^3J 7.6, 1H, H3″), 7.88 (ddd, $^3J = {}^3J = 7.6$, ^4J 1.8, 1H, H4′), 8.04 (dd, $^3J = {}^3J = 7.1$, 1H, H4″), 8.05 (d, ^3J 7.7, 1H, H3′), 8.38 (dd, ^3J 4.9, ^4J 1.1, 1H, H6″), 8.65 (d, ^3J 4.4, 1H, H6′).

[pypz$^{R(14)py}$] (3). Brown solid (77%). Elemental analysis: found: C, 76.8; H, 8.1; N, 10.8%. $C_{33}H_{42}N_4O$ requires C, 77.6, H, 8.3; N, 10.9%. ν_{max}(KBr)/cm^{-1}: 1614 ν(C=C + C=N), 788 $\gamma(CH)_{py}$. δ_H (300 MHz, DMSO-d^6, Me_4Si)/ppm: 0.84 (t, ^3J 6.9, 3H, CH_3), 1.23 (m, 22H, CH_2), 1.68 (m, 2H, CH_2), 3.95 (t, ^3J 6.4, 2H, OCH_2), 6.88 (d, ^3J 8.8, 2H, H_m), 7.13 (s, 1H, H4), 7.19 (d, ^3J 8.8, 2H, H_o), 7.38 (ddd, ^3J 7.6, ^3J 5.3,^4J 1.1, 1H, H5′), 7.46 (ddd, ^3J 7.4, ^3J 4.8,^4J 0.9, 1H, H5″), 7.72 (d, ^3J 8.0, 1H, H3″), 7.72 (ddd, $^3J = {}^3J = 7.7$, ^4J 1.8, 1H, H4′), 8.03 (dd, $^3J = {}^3J = 7.7$, 1H, H4″), 8.05 (d, ^3J 7.8, 1H, H3′), 8.38 (dd, ^3J 4.9, ^4J 1.1, 1H, H6″), 8.64 (d, ^3J 4.0, 1H, H6′).

[pypz$^{R(16)py}$] (4). Dark brown solid (81%). Elemental analysis: found: C, 77.8; H, 8.4; N, 9.9%. $C_{35}H_{46}N_4O$ requires C, 78.0; H, 8.6; N, 10.4%. ν_{max}(KBr)/cm^{-1}: 1613 ν(C=C + C=N), 786 $\gamma(CH)_{py}$. δ_H (300 MHz, DMSO-d^6, Me_4Si)/ppm: 0.84 (t, ^3J 6.9, 3H, CH_3), 1.23 (m, 26H, CH_2), 1.69 (m, 2H, CH_2), 3.95 (t, ^3J 6.4, 2H, OCH_2), 6.89 (d, ^3J 8.8, 2H, H_m), 7.15 (s, 1H, H4), 7.19 (d, ^3J 8.8, 2H, H_o), 7.42 (ddd, $^3J = 7.5$, ^3J 5.0, ^4J 1.1, 1H, H5′), 7.46 (ddd, $^3J = 7.4$, ^3J 4.9, ^4J 0.9, 1H, H5″), 7.73 (d, ^3J 8.0, 1H, H3″), 7.92 (ddd, $^3J = {}^3J = 7.6$, ^4J 1.7, 1H, H4′), 8.06 (dd, $^3J = {}^3J = 7.8$, 1H, H4″), 8.07 (d, ^3J 7.8, 1H, H3′), 8.39 (dd, ^3J 4.8, ^4J 1.1, 1H, H6″), 8.66 (d, ^3J 4.2, 1H, H6′).

[pypz$^{R(18)py}$] (5). Dark brown solid (83%). Elemental analysis: found:C, 78.1; H, 8.7; N, 9.6%. $C_{37}H_{50}N_4O$ requires: C, 78.4; H, 8.7; N, 9.9%. ν_{max}(KBr)/cm^{-1}: 1614 ν(C=C + C=N), 787 $\gamma(CH)_{py}$. δ_H (300 MHz, DMSO-d^6, Me_4Si)/ppm: 0.84 (t, ^3J 6.8, 3H, CH_3), 1.23 (m, 30H, CH_2), 1.69 (m, 2H, CH_2), 3.95 (t, ^3J 6.5, 2H, OCH_2), 6.88 (d, ^3J 8.8, 2H, H_m), 7.13 (s, 1H, H4), 7.19 (d, ^3J 8.8, 2H, H_o), 7.38 (dd, ^3J 6.9, ^3J 5.8, 1H, H5′), 7.46 (dd, ^3J 7.0, ^3J 5.0, 1H, H5″), 7.72 (d, ^3J 8.0, 1H, H3″), 7.88 (ddd, $^3J = 7.7$, ^4J 1.8, 1H, H4′), 8.03(dd, $^3J = {}^3J = 6.9$, 1H, H4″), 8.05 (d, ^3J 7.8, 1H, H3′), 8.38 (d, ^3J 4.2, 1H, H6″), 8.64 (d, ^3J 4.2, 1H, H6′).

Complexes [ZnCl$_2$(pypz$^{R(n)py}$)]; R(n) = ($C_6H_4OC_nH_{2n+1}$, n = 1, 12–18) (6–10)

To a solution of the corresponding pypz$^{R(n)py}$ in 20 mL of absolute ethanol was added $ZnCl_2$ in a 1 : 1 molar ratio, under nitrogen atmosphere (Scheme 1). The mixture was stirred for 24 h at room temperature, leading to the precipitation of a beige solid, which was filtered off, washed with *n*-hexane (10 mL) and dried *in vacuo* (0.05 hPa).

[ZnCl$_2$(pypz$^{R(1)py}$)] (6). Beige solid (8%). Elemental analysis: found: C, 50.6; H, 3.6; N, 12.1%. $C_{20}H_{16}N_4OZnCl_2$ requires C, 51.7; H, 3.5; N, 12.1%. ν_{max}(KBr)/cm^{-1}: 1608 ν(C=C + C=N), 789 $\gamma(CH)_{py}$. δ_H (see Results and discussion section).

[ZnCl$_2$(pypz$^{R(12)py}$)] (7). Beige solid (49%). Elemental analysis: found: C, 59.5; H, 6.0; N, 9.3%. $C_{31}H_{38}N_4OZnCl_2$ requires C, 60.2; H, 6.2; N, 9.0%. ν_{max}(KBr)/cm^{-1}: 1607 ν(C=C + C=N), 786 $\gamma(CH)_{py}$. δ_H (300 MHz, $CDCl_3$, Me_4Si)/ppm: 0.87 (t, ^3J 6.0, 3H, CH_3), 1.27 (m, 18H, CH_2), 1.84 (m, 2H, CH_2), 4.05 (t, ^3J 6.0, 2H, OCH_2), 6.93 (s, 1H, H4), 6.97 (d, ^3J 9.0, 1H, H3′), 7.06 (d, ^3J 9.0, 2H, H_m), 7.39 (m, 1H, H5′), 7.41 (d, ^3J 9.0, 2H, H_o), 7.57 (dd, $^3J = 7.5$, $^3J = 5.3$, 1H, H5″), 7.67 (ddd, $^3J = {}^3J = 8.1$, ^4J 1.8, 1H, H4′), 7.99 (d, ^3J 9.0, 1H, H3″), 7.98 (ddd, $^3J = {}^3J = 7.8$, ^4J 1.4, 1H, H4″), 8.78 (d, ^3J 4.5, 1H, H6′), 8.87 (d, ^3J 5.1, 1H, H6″).

[ZnCl$_2$(pypz$^{R(14)py}$)] (8). Beige solid (66%). Elemental analysis: found: C, 61.9; H, 6.9; N, 9.1%. $C_{33}H_{42}N_4OZnCl_2$ requires C, 61.3; H, 6.5; N, 8.7%. ν_{max}(KBr)/cm^{-1}: 1609 ν(C=C + C=N), 790 $\gamma(CH)_{py}$. δ_H (300 MHz, $CDCl_3$, Me_4Si)/ppm: 0.87 (t, ^3J 6.0, 3H, CH_3), 1.27 (m, 22H, CH_2), 1.84 (m, 2H, CH_2), 4.00 (t, ^3J 6.0, 2H, OCH_2), 6.87 (s, 1H, H4), 6.93 (d, ^3J 9.0, 1H, H3′), 7.01 (d, ^3J 9.0, 2H, H_m), 7.35 (m, 1H, H5′), 7.39 (d, ^3J 9.0, 2H, H_o), 7.50 (dd, $^3J = 7.6$, $^3J = 5.0$, 1H, H5″), 7.63 (ddd, $^3J = {}^3J = 8.0$, ^4J 1.8, 1H, H4′), 7.97 (d, ^3J 9.0, 1H, H3″), 8.01 (ddd, $^3J = {}^3J = 7.5$, ^4J 1.0, 1H, H4″), 8.74 (d, ^3J 4.6, 1H, H6′), 8.86 (d, ^3J 5.0, 1H, H6″).

[ZnCl$_2$(pypz$^{R(16)py}$)] (9). Beige solid (72%). Elemental analysis: found: C, 62.9; H, 7.2; N, 8.6%. $C_{35}H_{46}N_4OZnCl_2$ requires C, 62.3; H, 6.9; N, 8.3%. ν_{max}(KBr)/cm^{-1}: 1609 ν(C=C + C=N), 791 $\gamma(CH)_{py}$. δ_H (300 MHz, $CDCl_3$, Me_4Si)/ppm: 0.88 (t, ^3J 6.0, 3H, CH_3), 1.27 (m, 26H, CH_2), 1.85 (m, 2H, CH_2), 4.00 (t, ^3J 6.0, 2H, OCH_2), 6.91 (s, 1H, H4), 6.96 (d, ^3J 9.0, 1H, H3′), 7.00 (d, ^3J 9.0, 2H, H_m), 7.38 (m, 1H, H5′), 7.42 (d, ^3J 9.0, 2H, H_o), 7.55 (dd, $^3J = 7.4$, $^3J = 5.3$, 1H, H5″), 7.66 (ddd, $^3J = {}^3J = 8.3$, ^4J 1.5, 1H, H4′), 7.96 (d, ^3J 9.0, 1H, H3″), 8.00 (ddd, $^3J = {}^3J = 7.5$, ^4J 1.3, 1H, H4″), 8.77 (d, ^3J 4.3, 1H, H6′), 8.86 (d, ^3J 5.2, 1H, H6″).

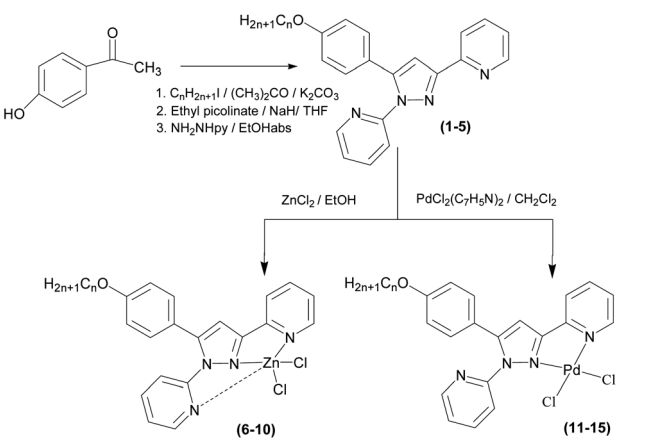

Scheme 1 Schematic synthesis of pypz$^{R(n)py}$ and [MCl$_2$(pypz$^{R(n)py}$)] (M = Zn, Pd).

[$ZnCl_2$(pypz$^{R(18)py}$)] (10). Beige solid (49%). Elemental analysis: found: C, 63.8; H, 7.7; N, 8.5%. $C_{37}H_{50}N_4OZnCl_2$ requires C, 63.2; H, 7.2; N, 8.0%. ν_{max}(KBr)/cm^{-1}: 1609 ν(C=C + C=N), 790 $\gamma(CH)_{py}$. δ_H (300 MHz, $CDCl_3$, Me_4Si)/ppm: 0.87 (t, ^3J 6.0, 3H, CH_3), 1.27 (m, 30H, CH_2), 1.84 (m, 2H, CH_2), 4.05 (t, ^3J 6.0, 2H, OCH_2), 6.93 (s, 1H, H4), 6.97 (d, ^3J 9.0, 1H, H3′), 7.06 (d, ^3J 9.0, 2H, H_m), 7.39 (m, 1H, H5′), 7.41 (d, ^3J 9.0, 2H, H_o), 7.57 (dd, ^3J = 7.6, ^3J = 5.3, 1H, H5″), 7.68 (ddd, ^3J = ^3J= 8.0, ^4J 1.7, 1H, H4′), 7.99 (d, ^3J 9.0, 1H, H3″), 8.04 (ddd, ^3J = ^3J = 7.7, ^4J 1.3, 1H, H4″), 8.78 (d, ^3J 4.6, 1H, H6′), 8.87 (d, ^3J 5.0, 1H, H6″).

Complexes [$PdCl_2$(pypz$^{R(n)py}$)]; R(n) = ($C_6H_4OC_nH_{2n+1}$, n = 1,12–18) (11–15)

To a solution of the corresponding pypz$^{R(n)py}$ in 20 mL of dicloromethane was added $PdCl_2(C_7H_5N)_2$ in a 1 : 1 molar ratio, under nitrogen atmosphere (Scheme 1). The mixture was stirred for 24 h at room temperature. The final mixture was vacuum concentrated yielding to the precipitation of a solid, which was filtered off, washed with *n*-hexane (10 mL) and dried *in vacuo* (0.05 hPa).

[$PdCl_2$(pypz$^{R(1)py}$)] (11). Yellow solid (54%). Elemental analysis: found: C, 47.0; H, 3.2; N, 11.0%. $C_{20}H_{16}N_4OPdCl_2$ requires C, 47.5; H, 3.2; N, 11.1%. ν_{max}(KBr)/cm^{-1}: 1609 ν(C=C + C=N), 786 $\gamma(CH)_{py}$. δ_H (see Results and discussion section).

[$PdCl_2$(pypz$^{R(12)py}$)] (12). Yellow solid (30%). Elemental analysis: found: C, 55.9; H, 5.4; N, 8.1%. $C_{31}H_{38}N_4OPdCl_2$ requires C, 56.4; H, 5.8; N, 8.5%. ν_{max}(KBr)/cm^{-1}: 1612 ν(C=C + C=N), 789 $\gamma(CH)_{py}$. δ_H (300 MHz, $CDCl_3$, Me_4Si)/ppm: 0.87 (t, ^3J 6.0, 3H, CH_3), 1.26 (m, 18H, CH_2), 1.73 (m, 2H, CH_2), 3.90 (t, ^3J 6.0, 2H, OCH_2), 6.78 (d, ^3J 9.0, 2H, H_m), 6.93 (s, 1H, H4), 7.12 (d, ^3J 9.0, 2H, H_o), 7.32 (d, ^3J 9.0, 1H, H3″), 7.43 (m, 1H, H5′), 7.45 (m, 1H, H5″), 7.74 (ddd, ^3J = ^3J = 7.8, ^4J 1.5, 1H, H4′), 7.84 (d, ^3J 9.0, 1H, H3′), 8.04 (dd, ^3J 7.5, ^3J 7.2, 1H, H4″), 8.61 (dd, ^3J 4.8, ^4J 1.2, 1H, H6″), 9.25 (d, ^3J 5.7, 1H, H6′).

[$PdCl_2$(pypz$^{R(14)py}$)] (13). Yellow solid (50%). Elemental analysis: found: C, 56.9; H, 5.9; N, 8.2%. $C_{33}H_{42}N_4OPdCl_2$ requires C, 57.5; H, 6.2; N, 8.1%. ν_{max}(KBr)/cm^{-1}: 1612 ν(C=C + C=N), 790 $\gamma(CH)_{py}$. δ_H (300 MHz, $CDCl_3$, Me_4Si)/ppm: 0.87 (t, ^3J 6.0, 3H, CH_3), 1.27 (m, 22H, CH_2), 1.73 (m, 2H, CH_2), 3.89 (t, ^3J 6.0, 2H, OCH_2), 6.79 (d, ^3J 9.0, 2H, H_m), 6.93 (s, 1H, H4), 7.12 (d, ^3J 9.0, 2H, H_o), 7.31 (d, ^3J 9.0, 1H, H3″), 7.43 (m, 1H, H5′), 7.44 (m, 1H, H5″), 7.74 (ddd, ^3J = ^3J = 7.8, ^4J 1.5, 1H, H4′), 7.85 (d, ^3J 9.0, 1H, H3′), 8.06 (dd, ^3J 7.5, ^3J 7.2, 1H, H4″), 8.62 (dd, ^3J 4.5, ^4J 1.5, 1H, H6″), 9.30 (d, ^3J 6.0, 1H, H6′).

[$PdCl_2$(pypz$^{R(16)py}$)] (14). Light yellow solid (98%). Elemental analysis: found: C, 58.3; H, 6.1; N, 8.0%. $C_{35}H_{46}N_4OPdCl_2$ requires C, 58.7; H, 6.5; N, 7.8%. ν_{max}(KBr)/cm^{-1}: 1609 ν(C=C + C=N), 779 $\gamma(CH)_{py}$. δ_H (300 MHz, $CDCl_3$, Me_4Si)/ppm: 0.87 (t, ^3J 6.0, 3H, CH_3), 1.26 (m, 26H, CH_2), 1.75 (m, 2H, CH_2), 3.90 (t, ^3J 6.0, 2H, OCH_2), 6.78 (d, ^3J 9.0, 2H, H_m), 6.94 (s, 1H, H4), 7.12 (d, ^3J 9.0, 2H, H_o), 7.32 (d, ^3J 9.0, 1H, H3″), 7.44 (m, 1H, H5′), 7.46 (m, 1H, H5″), 7.75 (ddd, ^3J = ^3J = 7.8, ^4J 1.5, 1H, H4′), 7.86 (d, ^3J 9.0, 1H, H3′), 8.05 (dd, ^3J = ^3J = 7.5, 1H, H4″), 8.61 (dd, ^3J 3.9, ^4J 0.9, 1H, H6″), 9.28 (d, ^3J 5.7, 1H, H6′).

[$PdCl_2$(pypz$^{R(18)py}$)] (15). Light yellow solid (49%). Elemental analysis: found: C, 59.8; H, 6.5; N, 7.1%. $C_{37}H_{50}N_4OPdCl_2$

Table 1 Crystal and refinement data for 1·H_2O, 6 and 11·CH_2Cl_2

	1·H_2O	6	11·CH_2Cl_2
Empirical formula	$[C_{20}H_{18}N_4O_2]$	$[C_{20}H_{16}Cl_2N_4OZn]$	$[C_{21}H_{16}Cl_4N_4OPd]$
Formula weight	346.38	464.64	588.58
Crystal system	Monoclinic	Monoclinic	Monoclinic
Space group	$P2_1/n$	$P2_1/c$	$C2/c$
a/Å	6.0659(7)	13.105(3)	11.693(2)
b/Å	15.261(2)	21.483(5)	13.833(2)
c/Å	19.086(2)	8.078(2)	28.947(3)
α/°	90°	90	90
β/°	98.971(2)°	103.413(4)	96.969(3)
γ/°	90°	90	90
V/Å^3	1745.2(4)	2212.1(9)	4647.6(7)
Z	4	4	8
T/K	293(2)	296(2)	296(2)
F(000)	728	944	2336
ρ_c/g cm^{-3}	1.318	1.395	1.682
μ/mm^{-1}	0.088	1.368	1.280
Scan technique	ω and φ	ω and φ	ω and φ
Data collected	(−7, −18, −21) to (6, 18, 21)	(−15, −24, −9) to (15, 25, 9)	(−14, −17, −33) to (12, 17, 36)
θ range/°	1.72 to 25.00	1.60 to 25.00	1.42 to 27.00
Reflections collected	13202	16529	20530
Independent reflections	3033 (R_{int} = 0.1215)	3876 (R_{int} = 0.1271)	5082 (R_{int} = 0.0741)
Completeness to maximum θ/%	98.9	99.4	100.0
Data/restraints/parameters	3033/0/236	3876/0/253	5082/3/269
Observed reflections [$I > 2\sigma(I)$]	1116	1322	2766
R^a	0.0674	0.0822	0.0513
$R_{wF}{}^b$	0.1876	0.2039	0.1487

^{a} $\Sigma[|F_o| - |F_c|]/\Sigma|F_o|$. ^{b} $\{\Sigma[w(F_o{}^2 - F_c{}^2)^2]/\Sigma[w(F_o{}^2)^2]\}^{1/2}$.

requires C, 59.7; H, 6.8; N, 7.5%. ν_{max}(KBr)/cm^{-1}: 1609 ν(C=C + C=N), 781 $\gamma(CH)_{py}$. δ_H (300 MHz, $CDCl_3$, Me_4Si)/ppm: 0.86 (t, ^3J 6.0, 3H, CH_3), 1.25 (m, 30H, CH_2), 1.74 (m, 2H, CH_2), 3.90 (t, ^3J 6.0, 2H, OCH_2), 6.79 (d, ^3J 9.0, 2H, H_m), 6.91 (s, 1H, H4), 7.14 (d, ^3J 9.0, 2H, H_o), 7.32 (d, ^3J 9.0, 1H, H3″), 7.44 (m, 1H, H5′), 7.46 (m, 1H, H5″), 7.76 (ddd, $^3J = {}^3J = 7.5$, $^4J = 1.8$, 1H, H4′), 7.82 (d, ^3J 9.0, 1H, H3′), 8.04 (ddd, $^3J = {}^3J = 7.8$, $^4J = 1.5$, 1H, H4″), 8.62 (dd, ^3J 4.8, ^4J 0.9, 1H, H6″), 9.30 (dd, ^3J 5.7, ^4J 0.6, 1H, H6′).

The new compounds were stable solids soluble in common organic solvents such as $CHCl_3$, CH_2Cl_2 or acetone, between others.

X-Ray data collection and structure refinement

Data collection for all compounds was carried out at room temperature on a Bruker Smart CCD diffractometer using graphite-monochromated Mo-Kα radiation (λ = 0.71073 Å) operating at 50 kV and 35 mA. In all cases, data were collected over a hemisphere of the reciprocal space by combination of three exposure sets. Each exposure was of 10 s for (**1**) and (**6**) and 20 s for (**11**) covered 0.3° in ω. The cell parameters were determined and refined by a least-squares fit of all reflections. The first 100 frames were recollected at the end of the data collection to monitor crystal decay, and no appreciable decay was observed. A summary of the fundamental crystal and refinement data is given in Table 1.

The structures were solved by direct methods and refined by full-matrix least-square procedures on F2 (SHELXL-97).[16] All non-hydrogen atoms were refined anisotropically.

All hydrogen atoms were included in their calculated positions and refined riding on the respective carbon atoms, except for compound (**1**) where the hydrogen atoms of the water molecule were located in a Fourier synthesis and fixed.

For compound (**6**), after refining, the presence of solvent residual electron density was detected as disordered atomic groups located in the void regions, and centered in sites among the molecule. The solvent molecule could not be modeled properly in none of the crystals, due to the poor spectra quality. The program SQUEEZE, a part of the PLATON[17] package of crystallographic software, was used to calculate the solvent disordered area and remove its contribution to the overall intensity data. An improvement was observed in all refinement parameters and residuals when this procedure was applied.

Results and discussion

Synthetic procedures

All the new compounds (**1–5**, **6–10**, **11–15**) described in this work are schematically presented in Table 2 including the numbering used for their identification.

The new dipyridylpyrazole ligands pypz$^{R(n)py}$ (R(n) = $C_6H_4OC_nH_{2n+1}$, n = 1, 12–18) (**1–5**) were prepared by condensation of the corresponding 1-(4-*n*-alkyloxyphenyl)3-pyridyl) propane-1,3-diones with 2-hydrazinopyridine. β-pyridinediketone precursors were generated through a two-step process involving alkylation of 4-hydroxyacetophenone followed by a Claisen condensation with ethyl picolinate (Scheme 1).

Table 2 Formulation and numbering of the compounds

Compound[a]	n	Number
pypz$^{R(n)py}$	1	**1**
	12	**2**
	14	**3**
	16	**4**
	18	**5**
[$ZnCl_2$(pypz$^{R(n)py}$)]	1	**6**
	12	**7**
	14	**8**
	16	**9**
	18	**10**
[$PdCl_2$(pypz$^{R(n)py}$)]	1	**11**
	12	**12**
	14	**13**
	16	**14**
	18	**15**

[a] R(n) = $OC_6H_4C_nH_{2n+1}$.

The complexes [MCl_2(pypz$^{R(n)py}$)] (M = Zn, Pd; R(n) = $C_6H_4OC_nH_{2n+1}$, n = 1, 12–18) (**1–15**) were obtained by reaction of the corresponding ligands with $ZnCl_2$ or $PdCl_2(C_7H_5N)_2$ as described in Scheme 1. The elemental analysis of the compounds agrees with the proposed molecular formula [MCl_2(pypz$^{R(n)py}$)].

Details for the synthesis of all ligands and complexes are given in the Experimental section. The molecular representations of Scheme 1 are made on the basis of the crystalline structures of pypz$^{R(1)py}\cdot H_2O$ (**1**·H2O), [$ZnCl_2$(pypz$^{R(1)py}$)] (**6**) and [$PdCl_2$(pypz$^{R(1)py}$)]·CH_2Cl_2 (**11**·CH2Cl2) (see Crystal structures section and ESI‡).

Spectroscopic studies

All the ligands and complexes were characterized by spectroscopic techniques (IR, and ^{1}H-, ^{13}C- and ^{15}N-NMR in solution as well as in the solid state), and in all cases the results agree with the proposed molecular formulations (see Experimental section).

IR spectra

The IR spectra in the 4000–400 cm^{-1} region in the solid state of the ligands and complexes show the characteristic bands of pyridine and pyrazole rings. In the complexes, those are scarcely modified with respect to the free ligands.

^{1}H- and ^{13}C-NMR spectra

The ^{1}H-NMR and ^{13}C-NMR spectra of [MCl_2(pypz$^{R(n)py}$)] (M = Zn, Pd; R(n) = $C_6H_4OC_nH_{2n+1}$; n = 1) were recorded in solutions of $CDCl_3$ and DMSO-d^6 (HMQC and HMBC) and in the solid state (CPMAS) (Tables 3 and 4).

The main feature from the ^{1}H-NMR spectra is related to the chemical shift values of the H6 protons from the two pyridine groups (H6′ and H6″) which allow to indicate the presence of both *N*-coordinated and *N*-uncoordinated pyridine substituent.

Table 3 ^{1}H-NMR chemical shifts (in ppm) and some coupling constants (in Hz) in solution for **1**, **6** and **11**[a]

	L	L	$PdCl_2L$		$PdCl_2L$	$ZnCl_2L$	$ZnCl_2L$
			DMSO-d^6 7.3×10^{-3} M				
Nuclei	DMSO-d^6 $8.8\ 10^{-2}$ M	$CDCl_3$	(49%)	(8%)	$CDCl_3$ 2.0×10^{-2} M	$CDCl_3$ 8.8×10^{-2} M	DMSO-d^6
H-4	7.14 (s)	7.15 (s)	7.52 (s)	7.70 (s)	6.91 (s)	6.96 (s)	7.14 (s)
H-3′	8.05 (d) $^3J = 7.5$	8.16 (d) ^{3}J = 9.0	8.30	8.03	7.81 (d) $^3J = 8.7$	6.97 (d) $^3J = 8.5$	8.05 (d) $^3J = 8.0$
H-4′	7.89 (ddd) $^3J = {}^3J = 7.5$ $^4J = 1.7$	7.76 (m)	7.92	8.07	7.76 (ddd) $^3J = {}^3J = 7.8$ $^4J = 1.8$	7.67 (ddd) $^3J = {}^3J = 7.8$ $^4J = 1.6$	7.89 (ddd) $^3J = {}^3J = 7.7$ $^4J = 1.7$
H-5′	7.38 (ddd) $^3J = 7.5$ $^3J = 4.5$ $^4J = 1.1$	7.26 (m)	7.69	7.75	7.44* (m)	7.37 (m) $^3J = {}^3J = 6.3$ $^4J = 2.2$	7.38 (ddd) $^3J = 6.6$ $^3J = 4.8$
H-6′	8.65 (d) $^3J = 4.5$	8.67 (d) $^3J = 6.0$	9.00 $^3J = 5.1$	8.95 $^3J = 5.6$	9.32 (d) $^3J = 5.7$	8.74 (d) $^3J = 4.2$	8.65 $^3J = 4.3$
H-3″	7.73 (dd) $^3J = 7.7$ $^3J = 8.0$	7.50 (d) $^3J = 9.0$	7.24	7.71	7.32 (d) $^3J = 7.8$	7.81 (d) $^3J = 7.8$	7.73 (d) $^3J = 8.0$
H-4″	8.04 (m)	7.76 (m)	8.30	8.23	8.04 (ddd) $^3J = {}^3J = 7.8$ $^4J = 1.5$	7.97 (ddd) $^3J = {}^3J = 7.5$ $^4J = 1.2$	8.04 $^3J = {}^3J = 7.7$ $^4J = 1.8$
H-5″	7.46 (ddd) $^3J = 7.2$ $^3J = 4.9$ $^4J = 0.8$	7.26 (m)	7.55	7.70	7.47* (m)	7.54 (ddd) $^3J = {}^3J = 6.3$ $^4J = 1.6$	7.46 (ddd) $^3J = 6.7$ $^3J = 5.0$
H-6″	8.39 (dd) $^3J = 4.9$ $^4J = 1.1$	8.46 (d) $^3J = 6.0$	8.51 $^3J = 3.7$	8.87 $^3J = 5.9$	8.62 (dd) $^3J = 5.1$ $^4J = 1.0$	8.82 (d) $^3J = 4.8$	8.39 (dd) $^3J = 4.8$ $^4J = 1.1$
H-*ortho*	7.22 (d) $^3J = 8.8$	7.25 (d) $^3J = 9.0$	7.19 $^3J = 8.6$	7.10 $^3J = 8.8$	7.16 (d) $^3J = 9.0$	7.40 (d) $^3J = 8.7$	7.22 (d) $^3J = 8.8$
H-*meta*	6.91 (d) $^3J = 8.8$	6.85 (d) $^3J = 9.0$	6.90 $^3J = 8.6$	6.86 $^3J = 8.6$	6.81 (d) $^3J = 9.0$	7.04 (d) $^3J = 8.7$	6.91 (d) $^3J = 8.8$
OCH3	3.77 (s)	3.82 (s)	3.73 (s)	3.84	3.79 (s)	3.91 (s)	3.77 (s)

[a] * These signals may be reverse.

As the ligands exhibit three potential coordinating positions, we have determined the manner in which the different positions are involved towards each metal fragment.

The ^{1}H-NMR spectra in $CDCl_3$ solution of Zn derivatives (**6–10**) exhibited a similar pattern which can be related to a type of complexes with a molecular structure analogous to that of $[ZnCl_2(pypz^{R(1)py})]$ (**6**) complex, whose crystalline structure has been solved by us and described in the present paper (Fig. 8). In these cases H6″ are the most shifted ones with respect to those of the free ligand. Similarly, all Pd complexes (**11–15**) in $CDCl_3$ solution exhibit a similar pattern, involving the protons of the coordinated pyridine group. However, in Pd complexes the H6′ and H6″ chemical shift coordination effects are reversed when comparing to those found in Zn complexes, so suggesting a different coordinating mode. The crystalline structure of (**11**), which is also solved in this work (Fig. 9), indicated a bidentate coordination around the Pd centre. Therefore, on the basis of a bidentate coordination of the ligand around the metal fragment, two isomers N2,N1′-(isomer A) (Fig. 2(a)) or N2,N1″-(isomer B) (Fig. 2(b)) can be proposed.

To shed some light to this proposal we recorded the ^{1}H-NMR spectra of $[ZnCl_2(pypz^{R(n)py})]$ (**6–10**) complexes in DMSO-d^6 solution finding out that only the signals corresponding to the free *N*,*N*,*N*-ligands (n = 1, 12–18) (**1–5**) were observed, indicating that the solvent originates decomposition. However the ^{1}H-NMR and ^{13}C-NMR spectra of $[PdCl_2(pypz^{R(1)py})]$ exhibited duplicity of all signals in agreement with the presence of the two proposed linkage isomers A and B (Fig. 2) which were found in a 49–8% relationship respectively. In addition, new signals from the free ligand (found in a 43% relationship) were also present, indicating again certain dissociation from the starting complexes (Table 5).

Influence of variables like chain length, time and temperature on the isomeric mixture of Pd complexes was followed by ^{1}H-NMR experiments. So it was observed that the A/B isomers ratio increased with the chain length, being in all cases the highest concentration for A (Table 5).

On the other hand, by comparison of ^{1}H-NMR results of freshly prepared samples with those obtained seven days later, an increase of the free ligand concentration and therefore a decrease of both linkage isomers was observed (Table 5). This result can be explained by considering the existence of an initial equilibrium between both A and B isomers and the free ligand (Scheme 2) which evolves over time to the decomposition of the less stable isomer B, releasing free ligand.

Table 4 ^{13}C-NMR chemical shifts (in ppm) and some coupling constants (in Hz) in solution and solid state for **1**, **6** and **11**

	L	L	$PdCl_2L$		$PdCl_2L$	$ZnCl_2L$	$ZnCl_2L$
			DMSO-d^6				
Nuclei	DMSO-d^6	CPMAS	(49%)	(8%)	CPMAS	$CDCl_3$	CPMAS
C-3	151.4	152.1	149.6	152.1	150.0	147.3	146.4
C-4	105.7 $^1J = 178.7$	106.1	106.2	104.9	100.2 (weak) 103.1	107.6 $^1J = 181.5$	107.8
C-5	144.2	145.0	146.0	146.0	147.8	147.3	144.7
C-2′	150.6	150.4	149.8	151.0	153.4	147.3 $^3J = 9.0$	144.7
C-3′	119.3 (br)	120.2	122.5	119.0	124.3	113.6 $^1J = 169.7$ $^3J = 7.2$	113.6
C-4′	136.4 $^1J = 166.3$	136.7	140.7	141.9	139.2	139.7 $^1J = 165.6$ $^3J = 6.4$	140.1
C-5′	126.4 $^1J = 159.7$ $^2J = 7.3$	124.4	125.1	124.8	124.3	124.0 $^1J = 167.9$ $^2J = {}^2J = 6.8$	124.3
C-6′	148.9 $^1J = 175.8$	149.5	149.1	152.2	141.3	149.4	148.3
C-2″	151.7	153.1	149.6	150.4	150.0	145.1 $^3J = 8.4$	143.1
C-3″	119.1 $^1J = 165.9$ $^3J = 6.6$	120.2	120.2	118.9	124.3	121.0 $^1J = 166.3$ $^3J = 7.2$	123.6
C-4″	138.6 $^1J = 165.5$ $^3J = 6.5$	139.8	138.2	140.1	137.8 (Weak) 136.9 (Weak)	139.4 $^1J = 166.4$ $^3J = 6.0$	138.2
C-5″	123.0 $^1J = 166.3$ $^2J = {}^2J = 7.4$	123.9	125.5	124.4	124.3	126.1 $^1J = 167.5$ $^2J = {}^2J = 6.8$	127.8
C-6″	147.7 $^1J = 179.7$	148.8	148.1	152.1	141.3	149.8	151.9
C-*ipso*	122.0 $^3J = {}^3J = 6.8$	121.6	119.7	123.0	118.9	120.0 $^3J = {}^3J = 8.0$	118.8
C-*ortho*	129.2 $^1J = 159.8$ $^3J = 7.3$	128.0	129.8 129.4	129.8	129.6 127.1 (Weak)	130.6 $^1J = 161.0$ $^3J = 7.5$	132.5 129.1
C-*meta*	113.2 $^1J = 160.8$ $^3J = 4.6$	109.4	113.6 113.5	113.9 113.3	114.8	115.0 $^1J = 161.5$ $^3J = 4.5$	116.1 111.7
C-*para*	158.7	159.8	159.6	159.6	160.7	161.6	162.6
OCH_3	54.6 $^1J = 144.6$	55.6	54.7	54.7	54.9 56.6	55.5 $^1J = 144.4$	57.4

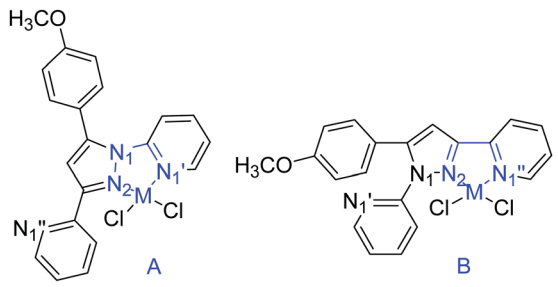

(a) (b)

Fig. 2 Possible linkage isomers for $[MCl_2(pypz^{R(1)py})]$ (M = Zn, Pd).

Finally the variable temperature spectra of $[PdCl_2(pypz^{R(1)py})]$(**11**) registered between 25 and 95 °C (Fig. 3) allow to establish at 65 °C the coalescence of the signals of both isomers, this result being clearly observed in the H6 and aromatic protons signals.

On the other hand in solid state, the ^{13}C-NMR data of **11** (Table 4) suggest the presence of two types of compounds on the basis of the duplicity of several of their C signals. This result was surprising, specially if we consider that the crystalline structure of the mentioned metal derivative shows the presence of a sole compound which exhibit a dimeric structure through a Pd–Pd interaction, in which each metal centre has the ligand N2,N1″-coordinated in a square-planar environment. The aliphatic chains of each moiety are *trans*- oriented so giving rise to a

Table 5 Evolution of the isomers ratio of $[PdCl_2(pypz^{R(n)py})]$ complexes by increasing the chain length and time

n	[ ]/M	% Isomer A	% Isomer B	% Ligand
Samples instantaneously registered in DMSO-d^6				
1	7.3×10^{-3}	49	8	43
12	1.5×10^{-2}	55	13	32
14	1.6×10^{-2}	63	11	25
16	1.6×10^{-2}	68	11	21
Samples registered after 7 days in DMSO-d^6				
1	7.3×10^{-3}	41	3	56
12	1.5×10^{-2}	46	6	48
14	1.6×10^{-2}	51	7	42
16	1.6×10^{-2}	57	9	34

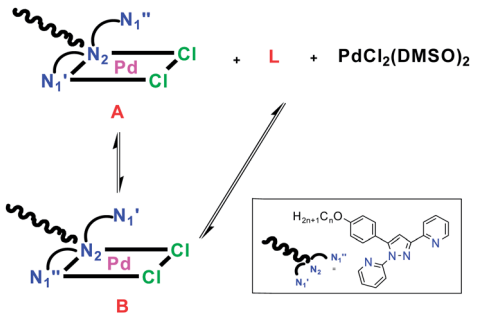

Scheme 2 Proposed equilibrium between A and B linkage isomers and the free ligand on DMSO-d^6 solution.

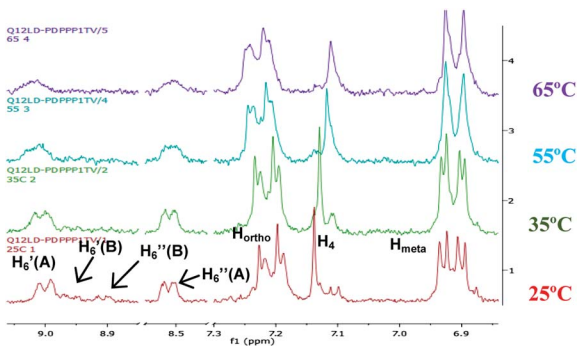

Fig. 3 Evolution of ^{1}H-NMR proton signals of $[PdCl_2(pypz^{R(1)py})]$ by increasing temperature.

head-to-tail or "Z"-shaped molecular configuration (Fig. 4(a)). However, a related head-to-head (or "U"-shaped) structure (Fig. 4(b)), probably less favourable to crystallize, should not be avoided.[18–21] On this consideration the presence of both "U"-shaped and "Z"-shaped binuclear stereoisomers in the solid state agree with ^{15}N-NMR results, as it will be described later.

This proposal was also supported by ^{1}H-NMR results obtained in $CDCl_3$ solution. So the metal–metal breaking, either of "Z" or "U" dimers, by non coordinating solvents as $CDCl_3$, should yield to the same monomeric form N2,N1″-coordinated

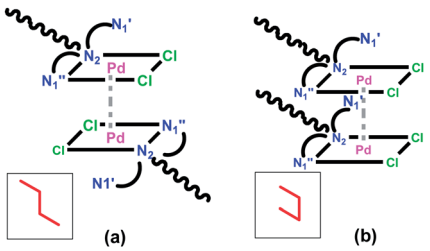

Fig. 4 "Z" – (a) and "U" – (b) shaped binuclear isomers of $[PdCl_2(pypz^{R(1)py})]$.

isomer B (Fig. 2(b)), which evolves to the N2,N1′-coordination observed for isomer A (Fig. 2(a)). By contrast, coordinating solvents like DMSO-d^6 induce substantial changes of the electronic density of the metal centre, allowing the formation of two different linkage isomers through a suggested five-coordinated intermediate $[PdCl_2(pypz^{R(1)py})(DMSO)]$.

^{15}N-NMR spectra

In order to confirm the above proposal as well as to deduce the coordinating form of the ligands in Zn and Pd complexes, ^{15}N-NMR studies of $pypz^{R(1)py}$ (**1**), $[ZnCl_2(pypz^{R(1)py})]$ (**6**) and $[PdCl_2(pypz^{R(1)py})]$ (**11**) as representative examples of each family were registered in $CDCl_3$, DMSO-d^6 and in the solid state (Table 6).

The Pd complex in DMSO-d^6 exhibits two signal pairs at −163.2 (N1) and −154.7 (N1″) ppm, and at −170.9 (N1) and −169.7 (N1′) corresponding to the linkage isomer A and isomer B respectively. The two N1 signals guarantee the presence of both isomers. Signals from N2 were not detected.

In addition, for the Pd complex, it was remarkable that the largest coordination chemical shifts ($\Delta\delta = \delta_{complex} - \delta_{ligand}$) were found for the pyridinic N1″ or N1′ nitrogens involved in the coordination ($\Delta\delta N1' = -93.5$ for A and $\Delta\delta N1'' = -75.1$ for B).

By contrast, the complex $[ZnCl_2(pypz^{R(1)py})]$ (which decomposes in DMSO-d^6) exhibits in $CDCl_3$ a single signal from N1 at −171.3 ppm in agreement with the presence of a sole species. The remaining δ signals at −132.7, −105.8, and −106.3 ppm are assigned to N2,N1′ and N1″ atoms respectively (Table 6). The

Table 6 ^{15}N-NMR chemical shifts (in ppm) in solution and solid state for **1**, **6** and **11**

	L	L	$PdCl_2L$		$PdCl_2L$	$ZnCl_2L$	$ZnCl_2L$
			DMSO-d^6				
Nuclei	DMSO-d^6	CPMAS	(49%)	(8%)	CPMAS	$CDCl_3$	CPMAS
N-1	−162.4	−164.7	−170.9	−163.2	−162.7	−171.3	−172.0
N-2	−104.8	−83.4	[a]	[a]	−159.7	−132.7	−132.0
N-1′	−76.2	−81.0	−169.7	[a]	−62.0	−105.8	−100.1
					−65.0		
N-1″	−79.6	−67.8	[a]	−154.7	−159.7	−106.3	−107.8

[a] Not detected values.

coordination chemical shifts of all N signals were almost equivalent of *ca* 28 ppm, this fact, suggesting a similar interaction between the Zn centre and each of the three coordinating nitrogens of the *N*,*N*,*N*-ligand.

In the solid state the Pd complex $[PdCl_2(pypz^{R(1)py})]$ exhibited two N1′ signals at −62.0 and −65.0 ppm in agreement with the presence of two "Z" and "U"-shaped binuclear stereoisomers above mentioned. These δ values were close to those of the free ligand so suggesting that the N1′ was not involved in the coordination to the metal centre.

However, the δ values of N2 and N1″ are −76.3 and −91.9 ppm shifted respect to the free ligand, supporting their participation in the coordination. The X-ray structure of $[PdCl_2(pypz^{R(1)py})]$ (**11**) confirms the foregoing features.

Similar deductions can be reached for $[ZnCl_2(pypz^{R(1)py})]$ (**6**) derivative.

In summary the ^{15}N-NMR studies allow to confirm that the Pd derivative $[PdCl_2(pypz^{R(1)py})]$ (**11**) presents two binuclear stereoisomers in the solid state in which the ligand was N2,N1″-coordinated. In DMSO-d^6 solution, duplicity of signals for N1 and single signals for N1′ and N1″ agree with the presence of two linkage isomers.

By contrast, only one species was found for $[ZnCl_2(pypz^{R(1)py})]$ (6) both in the solid state and in solution. In the first case a bidentate N2,N1″-coordination of the ligand was produced while, in the later, the three N atoms are interacting with the metal centre.

Crystal structures

Crystal structure of $[pypz^{R(1)py}]\cdot H_2O$ ($1\cdot H_2O$). Crystals of enough quality to be analyzed by X-ray diffraction analysis were grown for the ligand $pypz^{R(n)py}$ with $n = 1$. For long chained ligands all attempts of crystallization were proved to be unsuccessful.

A single crystal of the pyrazole $[(pypz^{R(1)py})]\cdot H_2O$ ($1\cdot H_2O$), was obtained by slow evaporation from a dichloromethane solution at room temperature. The compound crystallizes in monoclinic system, space group $P2_1/n$, with one molecule per asymmetric unit along with one water molecule (Table 1).

Table S1‡ lists the typical selected bond lengths and angles and the molecular structure is illustrated in Fig. 5.

The bond distances in the pyrazole, pyridine and benzene rings evidence a delocalized π system having this fact already been observed in related pyridine pyrazole ligands.[7,22] The two pyridine groups are arranged at the 1-and 3-positions of the pyrazole ring with their respective nitrogen atoms N1′ and N1″ at *trans*-position respect to the N2 of the pyrazole ring in order to minimize the interelectronic repulsions. The four rings are twisted each other with dihedral angles between 15.7(2)*y* 57.9(2)° respectively (Table S2†).

The water molecule is bonded to the pyrazole ring through hydrogen bonds involving the N2 atom of the pyrazolic group (d(N2···O2)) = 3.038 (5) Å, π(O2–H2A···N2) = 159.8°.

Each asymmetric unit is linked to the neighbouring one through coulombic interactions between the O atom of one water molecule and the N1′ of the pyridine at the 1-position (d = (O2···N1′) = 2.991(5) Å) (symmetry code: $1 + x, y, z$), giving rise to chains along the a axis (Fig. 6(a)). Furthermore, the adjacent chains are bonded through weak C–H···O interactions (d(O1–C15) = 3.39(1) Å) with an angle (C15–H15···O1) = 152.9° (symmetry code:$-x - 1, -y + 1/2, z + 1/2$) generating a double chain (Fig. 6(b)).

Additionally, $\pi\cdots\pi$ lateral interactions and C–H···N hydrogen bonds give rise to the formation of a 3D framework (Fig. 7).

Crystal structures of $[ZnCl_2(pypz^{R(1)py})]$ (6) and $[PdCl_2(pypz^{R(1)py})]\cdot CH_2Cl_2$ ($11\cdot CH_2Cl_2$)

Suitable crystals of compounds **6** and **11** were obtained by diffusion of hexane into a dichloromethane solution. Fig. 8 and 9 illustrate the perspective view of both compounds and Tables 7 and 8 list selected bond distances and angles for them. Both complexes (**6** and **11**) crystallise in the monoclinic system, space

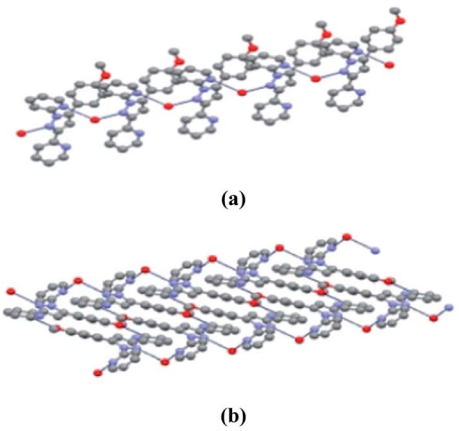

Fig. 6 Molecular chain (a) and double chain (b) along the *a* axis.

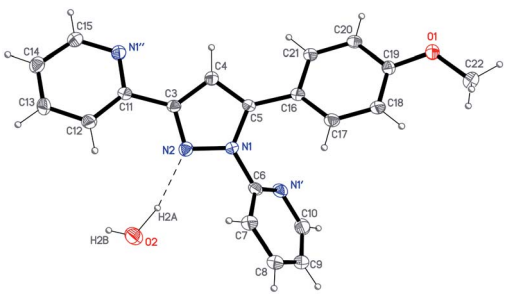

Fig. 5 ORTEP plot of $[(pypz^{R(1)py})]\cdot H_2O$ ($1\cdot H_2O$) with 20% probability.

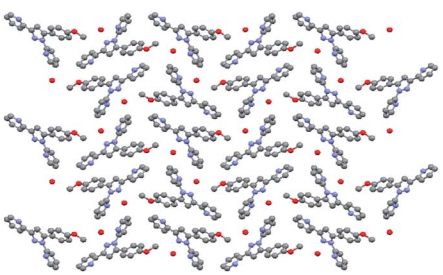

Fig. 7 3D framework through the a axis.

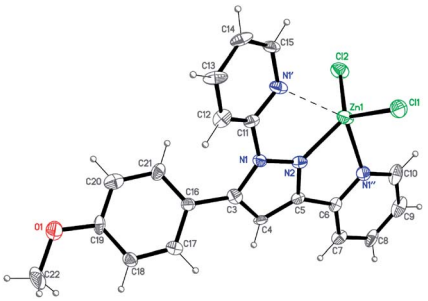

Fig. 8 ORTEP plot of $[ZnCl_2(pypz^{R(1)py})]$ (**6**) with 20% probability.

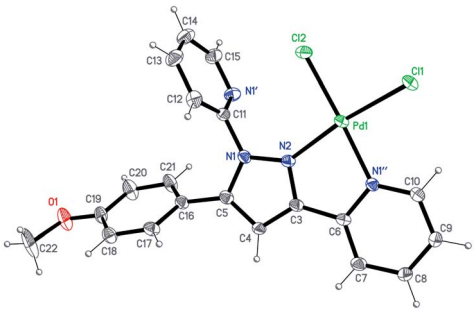

Fig. 9 ORTEP plot of $[PdCl_2(pypz^{R(1)py})]\cdot CH_2Cl_2$ (**11**$\cdot CH_2Cl_2$) with 20% probability. The dichloromethane molecule have been omitted for clarity.

Table 7 Selected bond distances (Å) and angles (°) for (**6**)

Zn – N2	1.997(8)	N2–Zn–N1″	74.0(3)
Zn–N1″	2.263(9)	N2–Zn–Cl1	117.7(2)
Zn–Cl1	2.205(3)	N2–Zn–Cl2	122.7(2)
Zn–Cl2	2.209(3)	N2–Zn–N1′	67.3(3)
Zn···N1′	2.62(2)	N1″– Zn–Cl1	106.8(2)
		N1″–Zn–Cl2	100.2(2)
		N1″–Zn–N1′	140.6(3)
		N1′–Zn–Cl1	97.5(2)
		N1′–Zn–Cl2	94.7(2)
		Cl2–Zn–Cl1	118.4(1)

Table 8 Selected bond distances (Å) and angles (°) for **11**$\cdot CH_2Cl_2$

Pd–N2	2.044(5)	N2–Pd–N1″	79.4(2)
Pd–N1″	2.046(5)	N2–Pd–Cl2	98.4(1)
Pd–Cl2	2.282(2)	N1″–Pd–Cl2	177.3(1)
Pd–Cl1	2.285(2)	N2–Pd–Cl1	172.6(1)
Pd···N1′	4.057(2)	Cl2–Pd–Cl1	88.76(6)

group $P2_1/c$ and $C2/c$ respectively, the second one as dichloromethane solvate (Table 1). Both of them present one molecule in the asymmetric unit.

In both structures (**6**) and (**11**) the $pypz^{R(1)py}$ ligand presents the pyridine rings at the 1- and 3-positions of the pyrazole core. The planes between the pyrazole ring and the coordinated pyridyl group at the 3-position are twisted at 6.4 (1) and 2.2 (1)° for compound (**6**) and (**11**) respectively giving rise to an almost planar molecular fragment. This fact is confirmed by the dihedral angles between the ZnN2C5C6N1″ (**6**) and PdN2C3C6N1″ (**11**) metallocycles and the pyrazole and pyridine planes (value 1–3°). By contrast, the dihedral angles between the phenyl and the pyridine (at the 1-position of the pyrazole ring) of 46.3(1)° for (**6**) and 70.1(1)° for (**11**) avoid the overall planarity of the molecule (Fig. 10(a) and (b)).

The Zn(II) center is five-coordinated by three N atoms from the two pyridine rings, the pyrazole ring and two chlorine atoms, with Zn–Cl1 and Zn–Cl2 distances of 2.205(3) Å and 2.209(3) Å respectively, and the Zn–N distances in the range of 1.997(8)–2.601(8) Å, being the Zn–N2 (1.997(8) Å) the shortest one. The geometry around the Zn(II) center could be considered as distorted trigonal bipyramidal with the basal plane described by the pyrazolic nitrogen and the 2 chlorine atoms while the axial sites are occupied by the pyridinic nitrogens (π(Cl2–Zn–Cl1) = 118.4(1)°; π(N1″–Zn–N1′) = 140.6 (3)°).

The palladium derivative (**11**) exhibits a square-planar coordination produced by 2-*cis* located chlorine ligands and two nitrogen atoms of the *N*,*N*,*N*-ligand giving rise to two short distances Pd–N2 of 2.044(5) and Pd–N1″ of 2.046(5) Å and one longer Pd–N1′ of 4.057(5) Å. Additionally, a Pd–Pd interaction of 3.55(1) Å between metallic centers of neighbouring molecules give rise to the formation of dimers. The molecular dimer adopts a "Z"-shaped conformation in which the pirazolic substituents of each monomer are *trans*-oriented. The uncoordinated pyridine and phenyl ring planes of each monomer are twisted with an angle of 70.1(1)° (Fig. 11).

The methoxy groups are almost perpendicular to their respective phenyl plane with their two arms pointing in opposite directions.

The molecular geometry of this compound can be considered similar to that reported by us for the dimer complex $[Ag(Hpz^{R(14)py})_2]_2[NO_3]_2$.[7]

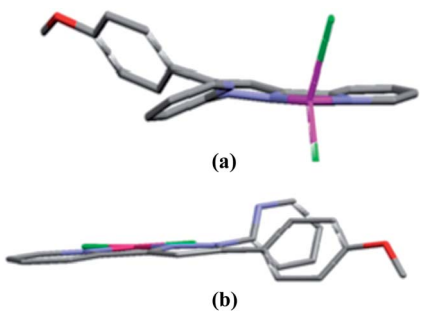

Fig. 10 View of the complexes (a) $[ZnCl_2(pypz^{R(1)py})]$ (**6**) and (b) $[PdCl_2(pypz^{R(1)py})]$ (**11**) showing the lack of planarity.

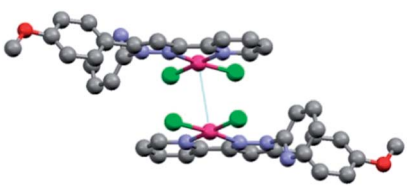

Fig. 11 Dimers of $[PdCl_2(pypz^{R(1)py})]$ (**11**) defined by Pd–Pd interactions.

Although several crystalline structures of Pd-complexes with a *cis*-$PdCl_2(L^2)$ core (L^2 = pyridylpyrazole type ligands) have been described in the literature,[23–27] from the best of our knowledge this is the first one of Pd–pyridylpirazole complexes exhibiting metal–metal interactions in a dimer.

On the other hand, in (**6**) the monomeric unities are arranged generating 1D double chains through weak non conventional hydrogen-bonding interactions C–H···O of ~3.4 Å and C–H···Cl of ~3.5 Å. These double chains are packed along the (1 0 1) direction (Fig. 12(a) and 13(a)).

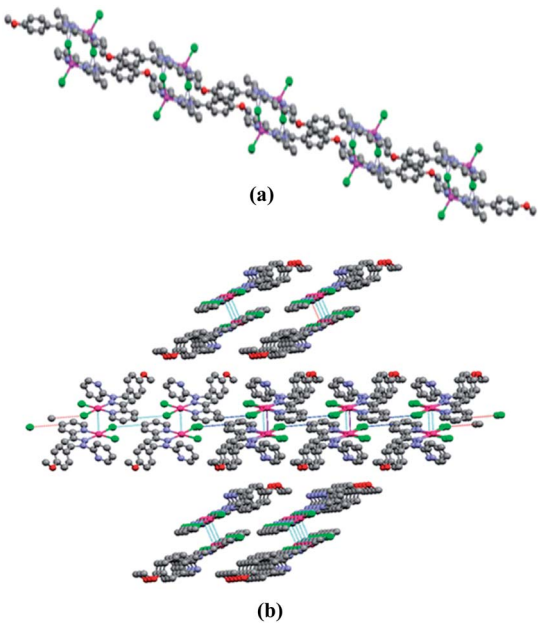

Fig. 12 (a) 1D chains parallel to the (1 0 1) direction for $[ZnCl_2(pypz^{R(1)py})]$ (**6**) and (b) crossed in the (1 0 1) and (−1 1 0) for $[PdCl_2(pypz^{R(1)py})]$ (**11**).

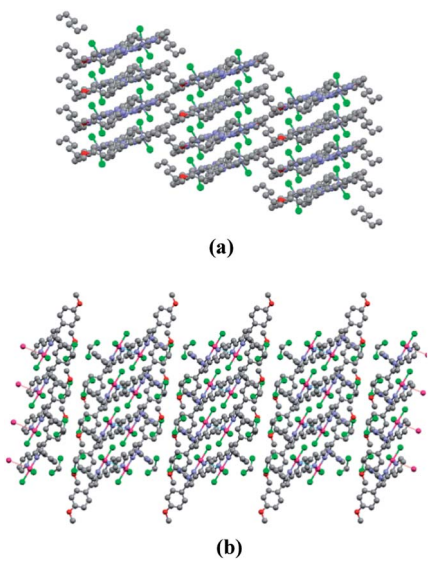

Fig. 13 Packings of (a) $[ZnCl_2(pypz^{R(1)py})]$ (**6**) and (b) $[PdCl_2(pypz^{R(1)py})]$ (**11**).

Table 9 Melting points of the compounds

Compound[a]	*n*	Melting point (°C)
$pypz^{R(n)py}$	12	70
	14	77
	16	78
	18	90
$[ZnCl_2(pypz^{R(n)py})]$	12	184
	14	161
	16	156
	18	155
$[PdCl_2(pypz^{R(n)py})]$	12	198
	14	199
	16	182
	18	196

[a] $R(n) = OC_6H_4C_nH_{2n+1}$.

In the case of (**11**) weak C–H···Cl interactions of ~3.6 Å between dimeric unities give rise to 1D chains which are crossed in the (1 0 1) and (−1 1 0) (Figs. 12(b) and 13(b)). New interactions between chains are not observed.

Thermal studies

The results obtained from POM observations and DSC studies of compounds **1–15** indicate that neither the $pypz^{R(n)py}$ ligands nor their Pd or Zn complexes are liquid crystalline compounds. The melting temperatures increased with the chain length for ligands and Pd derivatives, as expected, being the opposite variation observed for the Zn derivatives (Table 9).

The structural features related with the remarkable distortion of the planarity found in the compounds **1**, **6** and **11** with $n = 1$ determines a bulky whole molecular core which is also present in the related compounds containing longer chains substituents (**2–5**, **7–10**, **12–15**). Then we believe that this molecular core involve an inadequate width-to-length molecular ratio which appears to be responsible for the non achievement of the supramolecular ordering of the mesophases in agreement with the observed non mesomorphic behaviour of all the investigated compounds.

Conclusions

All ligands and complexes were not LC materials as deduced from their thermal behaviour, this result being associated to their inadequate molecular shape to reach the required ordering at the LC state.

The Zn complexes $[ZnCl_2(pypz^{R(n)py})]$ are mononuclear species according to the X-ray structure of $[ZnCl_2(pypz^{R(1)py})]$ (**6**). The ligand is coordinated to the metal centre through N2 and N1″ atoms and interacts with the third one (N1′) giving rise to a distorted trigonal bipyramidal geometry.

However, in $CDCl_3$ solution, the three N atoms of the revealed species interact with the metal in a similar fashion.

The Pd derivatives $[PdCl_2(pypz^{R(n)py})]$ were found as two "Z"- and "U"- shaped binuclear stereoisomers. In those, the bidentate N2,N1″-coordination with the third nitrogen (N1′) pointing

out, preserve the square planar environment at each Pd centre, allowing a Pd–Pd interaction between neighboring molecules to produce dimers. In the solid state the "Z"-shape was found in the crystalline structure of $[PdCl_2(pypz^{R(1)py})]\cdot CH_2Cl_2$ ($\mathbf{11}\cdot CH_2Cl_2$) while ^{13}C- and ^{15}N-NMR data evidenced the presence of the two forms.

In $CDCl_3$ solution the metal–metal interaction is broken yielding to a square planar molecular species which maintain the bidentate N2,N1′-coordination.

An equilibrium between N2,N1′′- and N2,N1′-coordinated species was proposed in DMSO-d^6 solution, so indicating the influence of the coordinating solvent to produce linkage isomers (probably through five-coordinated intermediate species).

Acknowledgements

Thanks are given to Ministerio de Economía y Competitividad (MINECO) of Spain for financial support (CTQ2010-16122 and CTQ2011-25172). L. S. thanks the Ministerio de Educación, Cultura y Deporte (Spain) for the predoctoral scholarship from the FPU program.

Notes and references

1 *Structure and Bonding*, ed. B. Donnio and D.W. Bruce, Springer, Berlin, Heidelberg, 1999, vol. 95, pp. 194–217; S. A. Hudson and P. M. Maitlis, *Chem. Rev.*, 1993, **93**, 861; P. Espinet, M. A. Esteruelas, L. A. Oro, J. L. Serrano and E. Sola, *Coord. Chem. Rev.*, 1992, **117**, 215; *Metallomesogens; Synthesis, Properties and Applications*, ed. J. L. Serrano, VCH, New York, NY, 1996; A. M. Giroud-Godquin and P. M. Maitlis, *Angew. Chem., Int. Ed. Engl.*, 1991, **30**, 375; A. M. Giroud-Godquin, *Coord. Chem. Rev.*, 1998, **178**, 1485.

2 M. Seredyuk, A. B. Gaspar, V. Ksenofontov, Y. Galyametdinov, J. Kusz and P. Guütlich, *J. Am. Chem. Soc.*, 2008, **130**, 1431; T. Cardinaels, J. Ramaekers, D. Guillon, B. Donnio and K. Binnemans, *J. Am. Chem. Soc.*, 2005, **127**, 17602; B. Donnio, D. Guillon, R. Deschenaux, D. W. Bruce, in *Comprehensive Coordination Chemistry II: From Biology to Nanotechnology*, ed. J. A. Mc Cleverty, J. J. Meyer, M. Fujita and A. Powel, Elsevier, Oxford, 2003, vol. 7, pp. 357–627; B. J. Coe and N. R. M. Curati, *Comments Inorg. Chem.*, 2004, **25**, 147.

3 M. C. Torralba, M. Cano, J. A. Campo, J. V. Heras, E. Pinilla, M. R. Torres, J. Perles and C. Ruiz-Valero, *J. Organomet. Chem.*, 2006, **691**, 2614.

4 M. C. Torralba, M. Cano, J. A. Campo, J. V. Heras, E. Pinilla and M. R. Torres, *J. Organomet. Chem.*, 2006, **691**, 765.

5 M. C. Torralba, J. A. Campo, J. V. Heras, D. W. Bruce and M. Cano, *Dalton Trans.*, 2006, 3918.

6 P. Ovejero, M. J. Mayoral, M. Cano, J. A. Campo, J. V. Heras, P. Fernández-Tobar, M. Valién, E. Pinilla and M. R. Torres, *Mol. Cryst. Liq. Cryst.*, 2008, **481**, 34.

7 P. Ovejero, E. Asensio, J. A. Campo, J. V. Heras, M. Cano, M. R. Torres, C. Núñez and C. Lodeiro, *Dalton Trans.*, 2013, **42**, 2107.

8 J. Casabó, J. Pons, K. S. Siddiqi, F. Teixidor, E. Molins and C. Miravitlles, *J. Chem. Soc., Dalton Trans.*, 1989, 1401.

9 J. Pons, X. López, J. Casabó, F. Teixidor, A. Caubet, J. Rius and C. Miravitlles, *Inorg. Chim. Acta*, 1992, **195**, 61.

10 J. Pons Picart, F. J. Sánchez, J. Casabó, J. Rius, A. Álvarez-Larena and J. Ros, *Inorg. Chem. Commun.*, 2002, **5**, 130.

11 J. Pons, F. J. Sánchez, J. Casabó, A. Álvarez-Larena, J. F. Piniella and J. Ros, *Inorg. Chem. Commun.*, 2003, **6**, 833.

12 V. J. Catalano and T. J. Craig, *Polyhedron*, 2000, **19**, 475.

13 V. J. Catalano and T. J. Craig, *Inorg. Chem.*, 2003, **42**, 321.

14 A. Satake, H. Koshino and T. Nakata, *J. Organomet. Chem.*, 2000, **595**, 208.

15 M. J. Mayoral, P. Cornago, R. M. Claramunt and M. Cano, *New J. Chem.*, 2011, **35**, 1020.

16 G. M. Sheldrick, *SHELX97, Program for Refinement of Crystal Structure*, University of Göttingen, Göttingen, Germany, 1997.

17 P. v. d. Sluis and A. L. Spek, *Acta Crystallogr., Sect. A: Found. Crystallogr.*, 1990, **46**, 194–201.

18 M. J. Mayoral, P. Ovejero, J. A. Campo, J. V. Heras, E. Pinilla, M. R. Torres, C. Lodeiro and M. Cano, *Dalton Trans.*, 2008, 6912.

19 M. J. Mayoral, P. Ovejero, J. A. Campo, J. V. Heras, M. R. Torres, C. Lodeiro and M. Cano, *New J. Chem.*, 2010, **34**, 2766.

20 C. K. Lee, K.-M. Hsu, C.-H. Tsai, C. K. Lai and I. J. B. Lin, *Dalton Trans.*, 2004, 1120.

21 K. Lee, H. H. Peng and I. J. B. Lin, *Chem. Mater.*, 2000, **16**, 530.

22 J. A. Campo, M. Cano, J. V. Heras, M. C. Lagunas, J. Perles, E. Pinilla and M. R. Torres, *Helv. Chim. Acta*, 2002, **85**, 1079; M. C. Torralba, M. Cano, J. A. Campo, J. V. Heras and E. Pinilla, *Z. Kristallogr.*, 2005, **220**, 617.

23 J. A. Perez, J. Pons, X. Solans, M. Font-Bardia and J. Ros, *Inorg. Chim. Acta*, 2005, **358**, 617.

24 M. D. Ward, J. S. Fleming, E. Psillakis, J. C. Jeffery and J. A. McCleverty, *Acta Crystallogr., Sect. C: Cryst. Struct. Commun.*, 1998, **54**, 609.

25 P. J. Steel, *Acta Crystallogr., Sect. C: Cryst. Struct. Commun.*, 1983, **39**, 1623.

26 D. A. House, P. J. Steel and A. A. Watson, *Aust. J. Chem.*, 1986, **39**, 1525.

27 V. Montoya, J. Pons, X. Solans, M. Font-Bardia and J. Ros, *Inorg. Chim. Acta*, 2005, **358**, 2763.

